SUPPORTING INFORMATION

Two-Stage Tunneling-Dominated Electrodeposition for Large-Scale Production of Ultralong Wavy Metal Microstructures on Native Oxide Layer-Passivated Si Electrode with Specific Surface Configuration

Yingjie Su,[‡] Hua Ren,[‡] Haiping Jiang, Shaochun Tang, Haiming Lu,* Xiangkang Meng*

National Laboratory of Solid State Microstructures, Collaborative Innovation Center of Advanced Microstructures, Institute of Materials Engineering, College of Engineering and Applied Sciences, Nanjing University, Nanjing 210093, China

*Address correspondence to these authors: haimlu@nju.edu.cn, mengxk@nju.edu.cn

Figure S1. A stitched image of the as-deposited ultralong Cu wavy microstructures (WMSs) obtained by electrodeposition and transferred on conductive adhesive tape.

Figure S2. (a) and (b) The SEM images of the resultant native oxide layer (NOL)-passivated highly doped *p*-type Si (p^+ Si) electrode. (c) and (d) Zoom-in focused ion beam (FIB) images of the characteristic features of the surface pattern corresponding to (a) and (b), respectively.

Figure S3. Optical microscopy image of the as-deposited Cu wavy microstructures.

Figure S4. Scanning electronic microscopy image of the forked AA-type Cu wavy microstructures.

Figure S5. The energy-dispersive X-ray spectroscopy data (elemental mappings, line-scan and spectrum) of one single hydrogen-reduced WMS (red color denotes oxygen, green color denotes copper, and blue color denotes silicon).

Figure S6. X-ray diffraction pattern of the microstructures with interconnected polyhedral nanoparticles.

Table S1. The peak location of Cu 2p scans after subsequently increasing etching times.

Table S2. The peak location of O 1s scans after subsequently increasing etching times.

Cu WMSs structure characterization. Scanning electron microscopy was performed on an FEI Quanta (FEI, USA). Hitachi FE–SEM S4800 microscope was used to determine the morphology, size, and distribution of the interconnected Cu polyhedral particles (Hitachi, Japan). X-ray diffraction measurements were carried out on a Rigaku Ultima III diffractometer with Cu Ka radiation (Rigaku, Japan). The chemical composition of the Cu WMSs was analyzed by X-ray photoelectron spectroscopy using a Thermo-VG Scientific ESCALab 250 Microprobe with a monochromatic Al Kα source (1486.6 eV). Depth profiling sputtering was performed by rasterring a 2.0 keV Ar^+ ion beam over a 2 × 4 mm^2 area of the sample at a medium current density (preset parameters of the equipment). Surface chemical composition analysis was performed on an energy dispersive spectrometer (Genesis XM2, EDAX, USA) attached to a field-emission scanning electron microscope (Nova NanoSEM 230, FEI, USA).

Electrical characterization of the Cu WMSs. Four-point probe resistivity measurements of typical segments of the Cu WMSs were performed by using a homemade system where Au electrode pad array are separated by 68 μm.

Figure S1 is the stitched image of two scanning electron microscopy (SEM) images for exhibiting dozens of as-deposited ultralong Cu wavy microstructures (WMSs) whose length reaches centimeter long. These WMSs were obtained by electrodeposition and transferred on conductive adhesive tape. One representative cm-long Cu WMS with some distinctive characters could be observed, and four of these distinctive characters were labeled by the colorful circles. The same one was examined by a series of SEM investigations as shown in the main text as **Figure 1** for determining its length and continuity. The colorful circle marks can be used to identify that the labeled WMSs are the same one. **Figure S2** (a) and (b) show the different types of surface pattern on lithographically patterned highly doped *p*-type Si (p^+ Si) electrode constructed by AA- and SA-type characteristic units; (c) and (d) are zoom-in focused ion beam (FIB) images of the AA- and

SA-type characteristic units, respectively. **Figure S3** shows the optical image of the as-deposited Cu WMSs. **Figure S4** shows the SEM image of the forked AA-type Cu WMS. The corresponding zoom-in SEM image of the labeled area is shown in **Figure 2c** in the main text. **Figure S5** shows the energy-dispersive X-ray spectroscopy data (elemental mappings, line-scan and spectrum) of one single hydrogen-reduced WMS (red color denotes oxygen, green color denotes copper, and blue color denotes silicon). **Figure S6** shows the XRD pattern of the microstructures with interconnected polyhedral nanoparticles. Three main diffraction peaks can be observed. The corresponding diffraction angles of the three peaks are 43.30, 50.43 and 74.13°, respectively. The miller indices of the three peaks are determined to be (111), (200) and (220) of face-centered cubic Cu (with space group $Fm\bar{3}m$, JCPDS 01-070-3039). A broad halo at 67.5−72.5° is ascribed to the patterned NOL-passivated p^+ Si electrode.

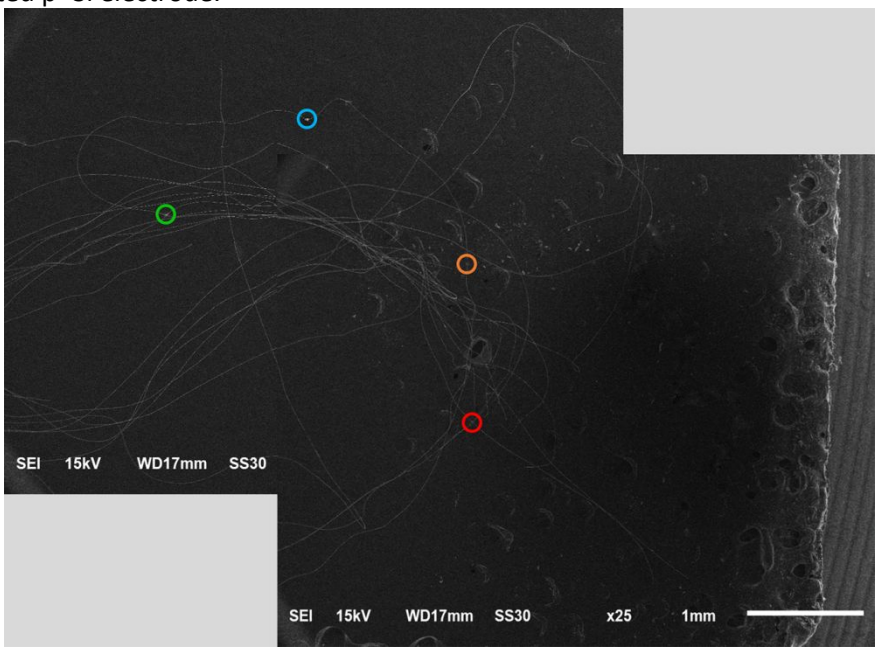

Figure 1. A stitched image of the as-deposited ultralong Cu wavy microstructures (WMSs) obtained by electrodeposition and transferred on conductive adhesive tape. The stitched image was stitched by two low-magnification scanning electron microscopy (SEM) images.

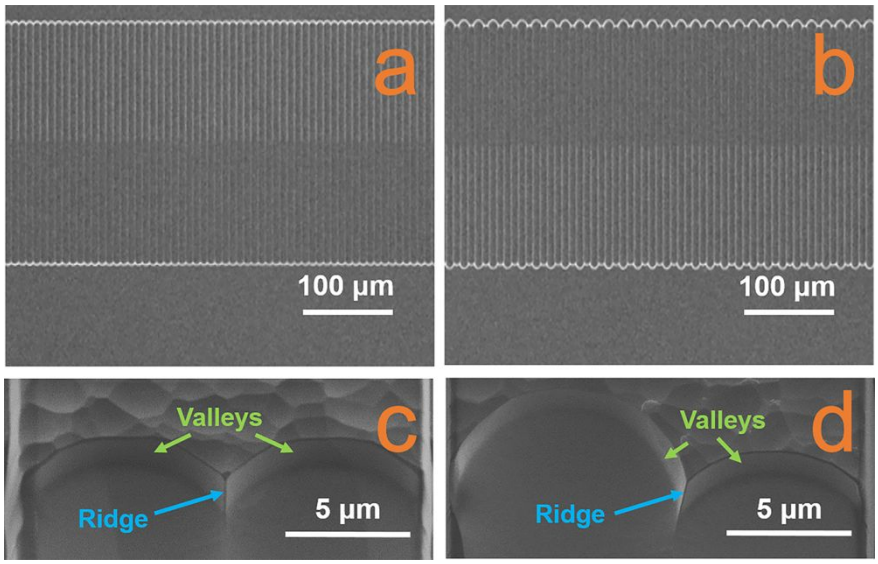

Figure 2. (a) and (b) The SEM images of the resultant native oxide layer (NOL)-passivated highly doped *p*-type Si (p^+ Si) electrode. (c) and (d) Zoom-in focused ion beam (FIB) images of the characteristic features of the surface pattern corresponding to (a) and (b), respectively.

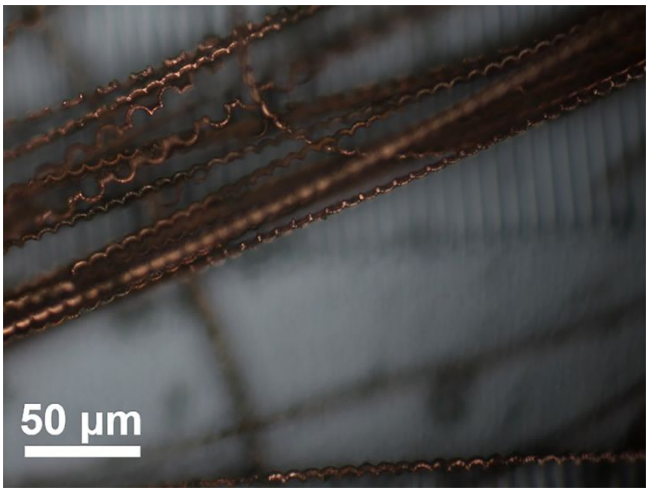

Figure 3. Optical microscopy image of the as-deposited Cu wavy microstructures.

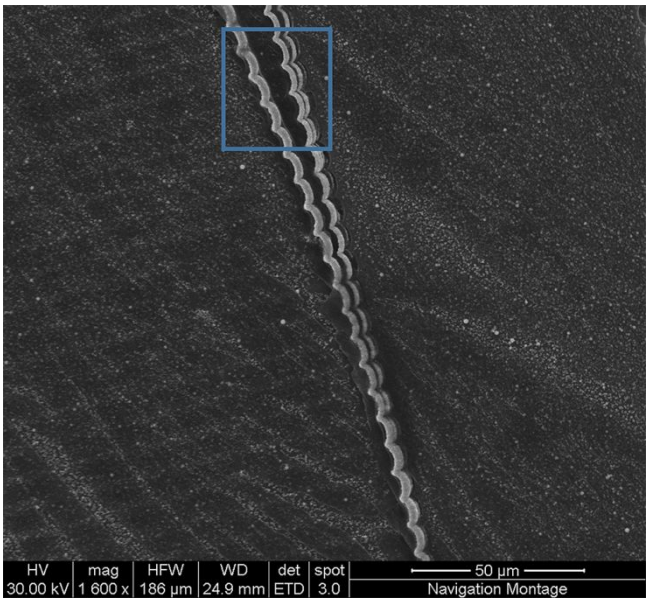

Figure 4. SEM image of the forked AA-type Cu wavy microstructure with 4 branches.

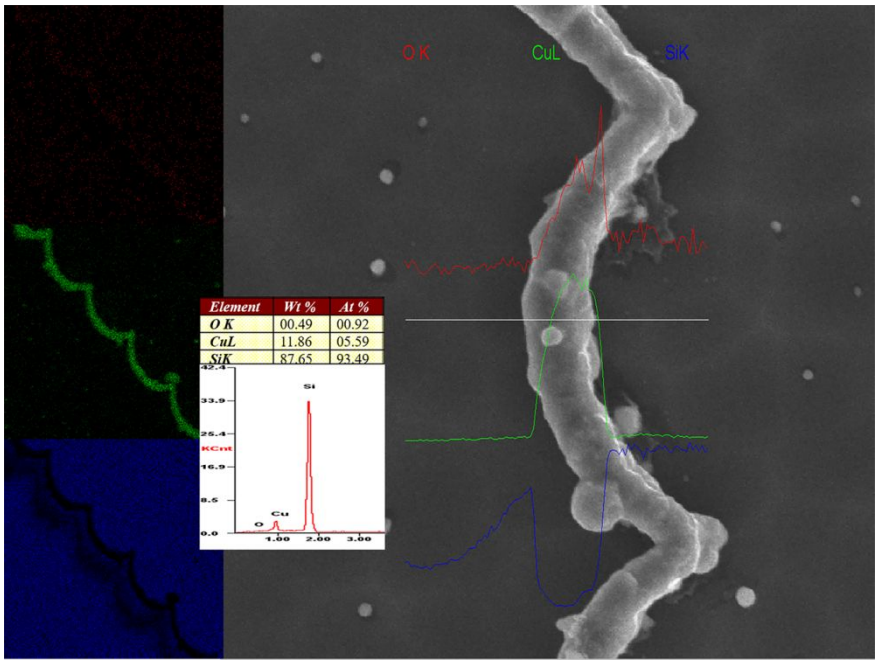

Figure 5. The energy-dispersive X-ray spectroscopy (EDX) data (elemental mappings, line-scan and spectrum) of one single hydrogen-reduced WMS (red color denotes oxygen, green color denotes copper, and blue color denotes silicon). Insert is the EDX spectrum of the sample and no more signals can be observed in the whole detected energy region (to 10 KeV, which was not fully shown in the insert).

Table S1 The peak location of Cu $2p_{3/2}$ scans after subsequently increasing etching times.

Etching time / Binding energy	500s	800s	1100s	1400s	1700s	2000s	2300s
932.78 eV	1	0.985994	0.996619	1	1	1	0.993204
932.68 eV	0.997482	1	1	0.980285	0.98297	0.997211	1

Table S2 The peak location of O 1s scans after subsequently increasing etching times.

Etching time / Binding energy	500s	800s	1100s	1400s	1700s	2000s	2300s
532.28 eV	0.971676	1	0.926428	0.884371	0.922492	1	0.914594
532.18 eV	0.991927	0.956264	1	0.942488	0.964525	0.94168	0.942091
532.08 eV	0.972638	0.982328	0.974296	1	0.982371	0.975322	0.948926
531.98 eV	0.973723	0.953343	0.974878	0.937912	0.909522	0.947773	1
531.88 eV	1	0.976626	0.949522	0.966237	1	0.986997	0.922432

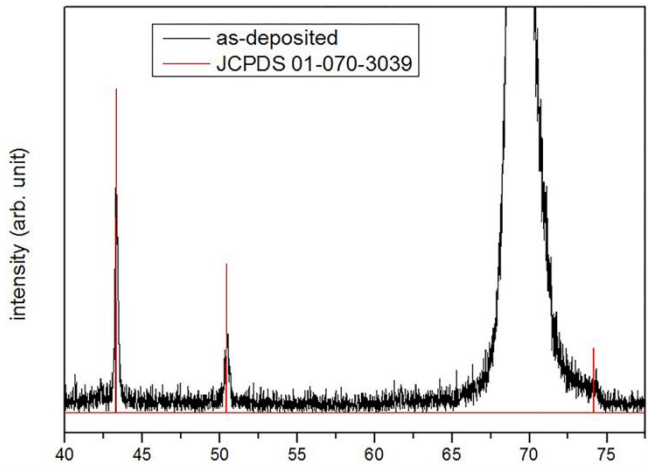

Figure 6. X-ray diffraction pattern of the microstructures with interconnected polyhedral nanoparticles.